Telophase disc: a new mammalian mitotic organelle that bisects telophase cells with a possible function in cytokinesis

PAUL R. ANDREASSEN[1,2], DOUGLAS K. PALMER[1], MARK H. WENER[3] and ROBERT L. MARGOLIS[1]

[1]*The Fred Hutchinson Cancer Research Center, 1124 Columbia Street, Seattle, WA 98104, USA*
Departments of [2]*Pathology and of* [3]*Laboratory Medicine and Medicine, University of Washington, Seattle, WA 98195, USA*

Summary

We have discovered a novel mitosis-specific human autoantigen that arises at the centromeres of prophase chromosomes, but ultimately participates in formation of an organelle that bisects the cell at late anaphase and during telophase. The organelle, discernible as a three-dimensional disc by confocal microscopy, encompasses the entire midzone diameter, and its distribution survives disassembly of interpolar microtubules by cold temperature treatment and detergent lysis of cells. Cytokinetic furrow contraction proceeds normally in dihydrocytochalasin B (DCB)-treated cells, and antigen distribution in the furrow is unaltered. In DCB, the furrow retracts in early interphase, coincident with loss of normal membrane association with the disc, resulting in the formation of binucleate cells. The midzone disc in both drug-treated and normal cells is present at the correct time and position to play a central role in cytokinesis. By immunocytochemistry, the disc appears to contain myosin but not actin. The position of the disc and the possible presence of myosin suggest that cytokinesis may involve the interaction of the disc organelle with actin in the cell cortex to produce cleavage in mammalian cells.

Key words: telophase disc, cytokinesis, mitosis.

Introduction

Interpolar microtubules from each half spindle overlap during anaphase and telophase in a region that defines the spindle midzone. Electron microscopy has shown an amorphous electron-dense matrix centered on the zone of overlap of anaphase interpolar microtubules (Buck and Tisdale, 1962; McIntosh and Landis, 1971). The midzone region of the anaphase spindle remains ill-defined with respect to morphology, constituents and function, although some antigens specific to the midzone region of the anaphase mitotic spindle have been reported. In each case, the antigen shows some apparent codistribution with microtubules, and ultimately becomes a midbody component (Cooke *et al.* 1987; Kingwell *et al.* 1987; Sellitto and Kuriyama, 1988).

Potential functions of the midzone elements include maintenance of the structural integrity of the anaphase spindle (Sellitto and Kuriyama, 1988), acting as an organizing platform for anaphase spindle motors (Wordeman *et al.* 1989), and imparting information on spindle position to the cell membrane in preparation for cell cleavage (Cooke *et al.* 1987). The distribution of a new mitosis-specific antigen, described here, suggests the anaphase spindle midzone may have yet another function: to serve in the creation of structures essential to the cell cleavage mechanism.

We have discovered a structure that forms at the position of the spindle equator in anaphase cells, expanding from this site to form a disc that bisects the two cell hemispheres just prior to telophase. This continuous three-dimensional disc appears to represent an organelle, since its integrity is not disturbed by the disassembly of microtubules, or by cell lysis. This novel structure, which we designate the 'telophase disc', was revealed by a human autoimmune serum which recognizes a mitosis-specific antigen of $60\times10^3\,M_r$. This antigen remains associated with separating chromatids until mid-anaphase, at which time it redistributes to the midzone of the spindle, and then deploys as a disc that fully partitions the anaphase cell at the spindle equator. Finally, the disc becomes constricted at the exact position of the cleavage furrow during telophase.

Given the position and extent of the telophase disc organelle in anaphase cells and given the response of cells to treatment with DCB, we propose that the telophase disc is centrally involved in the cytokinetic mechanism. Further, we find that the disc apparently contains cytoplasmic myosin. Therefore, it may contain mechanical elements for cell cleavage, which may interact with actin in the cell cortex to induce a contraction inward of the disc and cortex toward a central point.

Materials and methods

Cell culture and synchronization

Cells were kept in a humid incubator at 37°C with 5% CO_2. HeLa cells were grown as monolayers in Dulbecco's Modified Eagle's Medium (Gibco Laboratories, Grand Island, NY) supplemented

with 5% defined bovine calf serum (Hyclone Laboratories, Logan, UT). Human lymphoma cells (designated MANCA) derived from a patient with non-Hodgkin's lymphoma (Nishikori *et al.* 1984) were grown in suspension using RPMI 1640 (Gibco Laboratories) supplemented with 5% calf serum. Nocodazole (Sigma Chemical Co., St. Louis, MO) was used at 0.040 $\mu g\,ml^{-1}$ for HeLa cells and 0.080 $\mu g\,ml^{-1}$ for the lymphoma cells to block cells at the onset of mitosis.

Immunofluorescence microscopy

HeLa cells were grown a minimum of 12 h on polylysine-coated glass coverslips. Unless otherwise noted, cells were fixed 20 min with 2% paraformaldehyde in PBS (136 mM NaCl, 2 mM KCl, 10.6 mM Na_2HPO_4, and 1.5 mM KH_2PO_4 at pH 7.4) at 37°C. Cells were then washed with PBS, permeabilized 3 min with 0.2% Triton X-100 in PBS, and washed 3 times with PBS. Primary and secondary antibodies were applied in PBS containing 3% bovine serum albumin, 0.05% Tween 20 and 0.1% azide. Human sera were diluted 500-fold, mouse anti-β-tubulin (Eastacres Biologicals, Southbridge, MA) was diluted 50-fold, and mouse anti-myosin was used at 25 $\mu g\,ml^{-1}$. The anti-myosin antibody 2.42 was generated against *Acanthamoeba* myosin II and is specific for myosin in HeLa cells (D. Kaiser, personal communication; also our results (data not shown)). Incubation with primary antibodies (60 min in a humid chamber at 37°C) was followed by three washes with PBS. FITC-conjugated affinity-purified goat anti-human and anti-mouse, and Texas Red-conjugated goat anti-mouse secondary antibodies (Tago Inc., Burlingame, CA), were applied at 8.5 $\mu g\,ml^{-1}$ and 14 $\mu g\,ml^{-1}$ respectively, for 30 min. Where used, FITC–phalloidin (Sigma) was included at 3 $\mu g\,ml^{-1}$ with secondary antibody incubations. Coverslips were washed twice with PBS both before and after a 5 min incubation with propidium iodide (1 $\mu g\,ml^{-1}$ in PBS), or three times with PBS if propidium iodide staining was omitted. Coverslips were mounted with 25 mg ml^{-1} 1.4-diazabicyclo (2.2.2) octane (Johnson *et al.* 1982) (Kodak, Rochester, NY) in 90% glycerol and PBS at pH 8.6.

Samples were observed using a MRC-500 Laser Scanning Confocal Microscope (Bio-Rad Microscience, Cambridge, MA) with a Nikon Optiphot (Nikon, Inc., Torrance, CA). Photographs were taken on TMAX 100 film (Kodak) at f5.6 for one second. Prints were made on Ilford MC Rapid paper (Ilford Limited, Cheshire, England). Color photographs were taken on Kodak Gold 100 film (Kodak) and processed commercially.

Chromosome spreads

HeLa cells grown on coverslips were blocked 5–15 h in nocodazole and then swollen (5 min, 22°C) in 10 mM Tris–HCl (pH 7.4), 10 mM NaCl, and 5 mM $MgCl_2$ (Earnshaw *et al.* 1984). The coverslips were then centrifuged for 2.5 min at 2800 revs min^{-1}, washed twice in PBS, and processed for immunofluorescence as described above. Specific anti-CENP-B antibody was kindly provided by W. Earnshaw.

Immunofluorescence of chilled and permeabilized cells

For experiments in which microtubules were depolymerized by cold treatment, coverslips were treated first with polylysine and then for 1 h with 0.01% collagen (Sigma). HeLa cells were grown for 48 h prior to application of nocodazole for 12 h. Coverslips were then washed with nocodazole-free medium and incubated for 65 min at 37°C to yield anaphase- and telophase-enriched populations. The coverslips were then incubated on ice for 30 min (in medium prechilled to 4°C), fixed in paraformaldehyde/PBS for 20 min at 4°C, and processed for immunofluorescence as described above.

For detergent lysis of cold-treated cells, nocodazole-arrested HeLa cells were collected by shakeoff, washed with nocodazole-free medium, and placed in suspension culture at 5.0×10^5 cells ml^{-1}. After 65 min, cells were collected by centrifugation (120 *g*, 5 min), resuspended (5×10^5 cells ml^{-1}) in medium pre-chilled to 4°C, and incubated on ice for 30 min. Chilled cells were collected by centrifugation (4°C), and resuspended in 85 mM Pipes, 1 mM EGTA, 0.2% Triton X-100, 0.1% β-mercaptoethanol and 1 mM PMSF (phenylmethylsulfonyl fluoride) at pH 8.5. After 10 min, cells were pelleted and gently resuspended in fixative at 4°C for 20 min, and processed for immunofluorescence.

Dihydrocytochalasin B treatment of cells

HeLa cells grown on polylysine-coated coverslips were blocked for 12–16 h in nocodazole and released by washing with fresh culture medium. Dihydrocytochalasin B (DCB; Sigma), was immediately added to 10 μM from a 1000× stock in methanol. After 75 min, the cells were fixed in paraformaldehyde/PBS and processed for immunofluorescence as described above.

To quantify cytokinesis in the presence of DCB, HeLa cells growing on coverslips were blocked twice (16 h block, 8 h release, 16 h block) with 10 mM thymidine (Sunkara *et al.* 1979), and then released from thymidine block into nocodazole. After 12 h, cells were released into nocodazole-free medium and DCB was added to 2 μM. Control cells were released from nocodazole into fresh medium containing 0.02% methanol. At various time intervals, cells were fixed and processed for immunofluorescence. Synchronization yielded an initial mitotic population of about 80%. At later time points, cells containing midbodies (exclusion zone visible) detected by JH serum and complete furrows (furrowed membrane attached to midbody) were counted. Cells containing two nuclei and no discontinuity of cytoplasmic RNA, as determined by propidium iodide staining, were recorded as binucleate. In the typical experiment, three counts of 100 total cells were averaged for each coverslip using a Leitz Ortholux 2 microscope equipped for epifluorescence.

Chromosome isolation and immunoblotting

MANCA cells were blocked with nocodazole for 15 h and collected by centrifugation. Chromosomes were isolated by the polyamine method of Lewis and Laemmli (1982), with 0.1% β-mercaptoethanol, 2 $\mu g\,ml^{-1}$ PMSF, and 0.15 $\mu g\,ml^{-1}$ aprotinin included in all solutions from cell lysis through dilution of Percoll gradient fractions containing chromosomes. Chromosomes were pelleted (1400 *g*, 45 min), and then washed twice and resuspended in 5 mM Tris–HCl (pH 7.4) with 2 mM KCl, 0.25 mM spermidine, 0.15 $\mu g\,ml^{-1}$ aprotinin and 2 $\mu g\,ml^{-1}$ leupeptin. The chromosomes were essentially free of cytoplasmic debris and nuclei, as judged by phase-contrast microscopy and Hoechst staining.

Micrococcal nuclease was added to the chromosome suspension to 40 units ml^{-1}, and digestion (30 min, 37°C) was initiated by the addition of $CaCl_2$ to 1 mM. Digestion was stopped by the addition of EDTA (pH 7.4) to 10 mM, and insoluble material was removed by centrifugation. Samples of the supernatant fraction were placed in SDS sample application buffer, heated to 100°C for 5 min, and electrophoresed in 8% SDS–polyacrylamide gels (Sheir-Neiss *et al.* 1978) formed in a BioRad mini protean II gel apparatus. Resolved proteins were transferred to nitrocellulose (BA83; Schleicher and Schuell Inc., Keene, NH) for 2 h at 60 V in a buffer containing 25 mM Tris, 192 mM glycine and 40% methanol (Towbin *et al.* 1979). Western transfers were blocked for 30 min with PBS containing 0.1% non-fat powdered milk, 0.05% Tween 20 and 0.1% azide, and incubated overnight with JH serum diluted 1000-fold in blocking solution. Blots were washed with milk/PBS/Tween, milk/2 M NaCl/PBS, and again in milk/PBS/Tween. Following application of ^{125}I-labelled protein A (New England Nuclear, Boston, MA), blots were washed as above, dried, and autoradiographed at −70°C using an intensifying screen and Kodak XAR-5 film (Kodak).

Antibodies to the $60\times10^3 M_r$ antigen (TD-60) were affinity purified from Western transfers of chromosomal proteins to nitrocellulose. Antibodies were eluted with 50 mM glycine–HCl, pH 2.3; the pH of the eluate was neutralized by the addition of 50 mM potassium phosphate buffer, pH 7.7; and antibodies were concentrated with centricon small volume concentrators (Amicon, Danver, MA).

Results

Distribution of mitotic matrix antigens

Indirect immunofluorescence staining of HeLa cells using

human autoimmune serum JH is mitosis-specific, and shows a highly unusual series of redistributions at different stages of mitosis. In prophase cells bright spots (Fig. $1A_1,A_2$), which are localized to centromeres (see below), arise on condensing chromosomes. There is also fainter, more diffuse staining elsewhere on the chromosomes at prophase. The antigen remains enriched in foci on chromosomes through metaphase and into early anaphase (Fig. $1B_1,B_2$). By mid-anaphase, the antigen is concentrated in a series of narrow bars at the spindle midzone in a region restricted to the lateral spread of the two chromatid sets (Fig. $1C_1,C_2$). By late anaphase (the progression through anaphase is demonstrated by the position of the chromosomes throughout Fig. 1), the antigen, now absent from chromosomes, appears as a series of bars across the full midzone diameter of the cell with the outer edge of the staining closely apposed to the plasma membrane (Fig. $1D_1,D_2$). Less-intense staining of antigen is also visible interstitial to the bars. During telophase (Fig. $1E_1,E_2$), we observe an equatorial disc spanning the developing furrow. Where it meets the membrane, the antigen is contoured into cups centered on the apex of the furrow. The bars of antigen become increasingly condensed as telophase progresses. When the furrow is complete, staining is restricted to the midbody (Fig. $1F_1,F_2$). Fluorescence is absent from the central dark band visible in the midbody by phase-contrast microscopy. Control cells treated with normal human serum and/or secondary antibody alone give no detectable signals by epifluorescence or confocal microscopy. In interphase cells, only a weak and diffuse nuclear signal ranging from 0 % to <10 % of prophase nuclear signal is detected by JH antibodies (as quantified by pixel intensity averaged for the nuclear area).

The localization of fluorescence to discrete foci at the inner edge of chromosome rings in prometaphase cells (Fig. $1A_1,A_2$), suggested an association of the antigen with mitotic centromeres, which was confirmed by immunofluorescence analysis of chromosome spreads. Each chromosome contains a focus of staining that coincides with the centromere, and which can in some cases be resolved into closely spaced doublet foci (Fig. $2A_1,A_2$, Fig. 3B), as determined by computer superimposition of the antigen image with the whole chromosome image (visualized with propidium iodide). We have determined that the focal staining also coincides with the position of the centromeric protein CENP-B (Earnshaw *et al.* 1987) using a double label with a monospecific monoclonal antibody to CENP-B (data not shown). Although the arms of sister chromatids become more loosely associated during prophase arrest (Lima-de-Faria, 1955), such treatment has no effect on

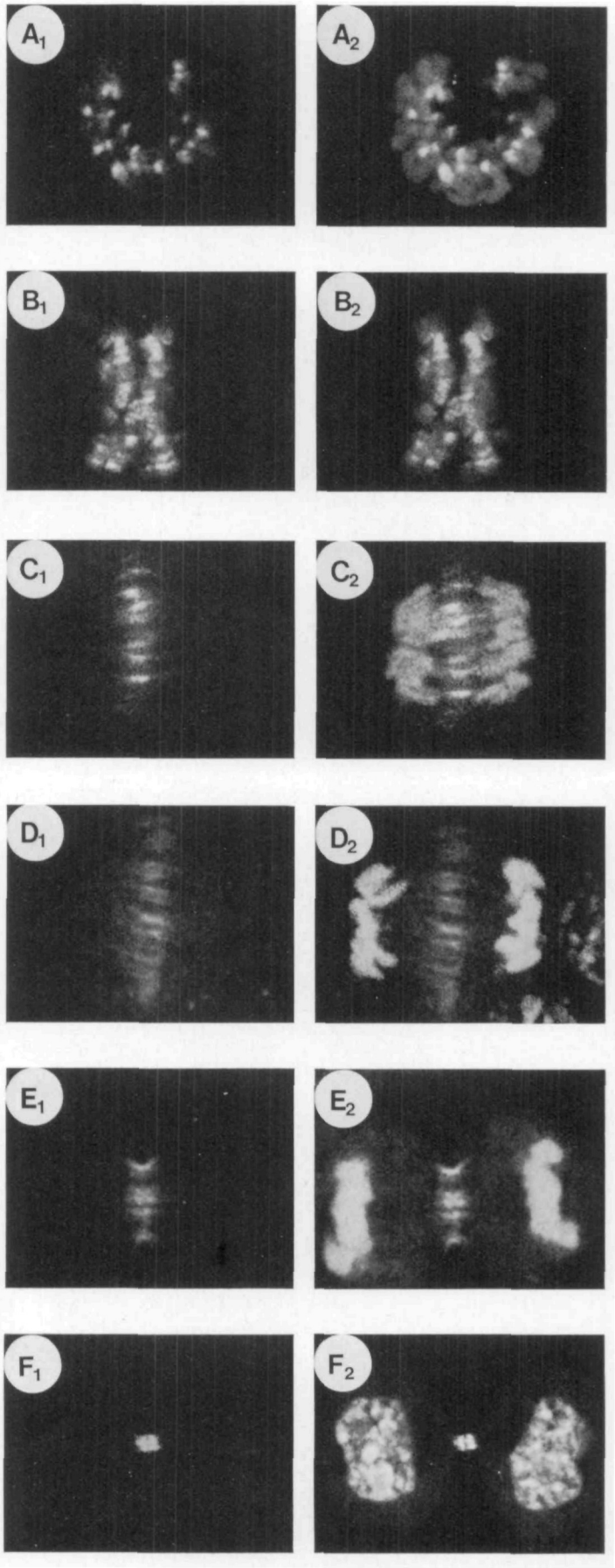

Fig. 1. Immunofluorescence localization of serum JH antigen in mitotic HeLa cells. HeLa cells were released from 12 h of mitotic arrest in 0.040 $\mu g\,ml^{-1}$ nocodazole, permitted to recover for 60 min at 37 °C, then fixed and processed for immunofluorescence. The redistribution of the antigen within the cell at different stages of mitosis is evident. Cells are shown at prometaphase (A_1,A_2), early anaphase (B_1,B_2), mid-anaphase (C_1,C_2), late anaphase (D_1,D_2), mid-telophase (E_1,E_2), and fully cleaved with a midbody bridge (F_1,F_2). All images in the left-hand column represent the antigen detected by serum JH, using fluorescein-conjugated goat anti-human secondary antibodies. Corresponding images of DNA in these same cells, visualized with propidium iodide, are shown merged with the image for serum JH in the right-hand column. All images are horizontal optical sections through the middle of the cells, generated by confocal microscopy. ×1200.

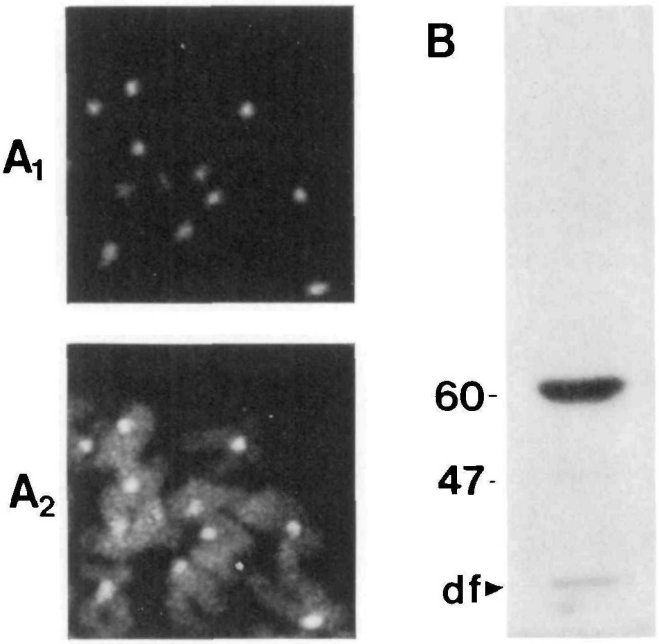

Fig. 2. Identification of the major serum JH antigen as a protein of $60\times10^3 M_r$ (TD-60) and its localization to centromeres in chromosome spreads. (A) Chromosome spreads were prepared from nocodazole-arrested mitotic HeLa cells by hypotonic cell lysis, and centrifugation of released chromosomes onto coverslips. Serum JH recognizes a single discrete focus on chromosomes, which corresponds to the primary constriction. Antigen recognized by serum JH, using FITC–goat anti-human secondary antibody (A_1); the same field, in which the image for whole chromosomes visualized with propidium iodide is merged with the image for serum JH (A_2). (B) Purified chromosomes were also subjected to Western blot analysis, and probed with serum JH antibody. A predominant band of $60\times10^3 M_r$ is detected, and a faint signal at $47\times10^3 M_r$ is also sometimes apparent. The dye front (df) is indicated by an arrowhead.

localization of the antigen(s) described here (data not shown).

Serum JH detects a strong band of $60\times10^3 M_r$ on Western blots of chromosomes isolated from cells arrested with nocodazole (Fig. 2B), whereas control normal human sera and other autoimmune sera do not detect this band. In addition to the $60\times10^3 M_r$ band, a weak band is also detected occasionally at $47\times10^3 M_r$ (Fig. 2B). This band is not consistently present, and its relationship to the $60\times10^3 M_r$ band is unknown. The $60\times10^3 M_r$ band, and no other, is also detected consistently in whole mitotic cell lysates.

We have affinity purified the antibody recognizing either the $60\times10^3 M_r$ or the $47\times10^3 M_r$ antigens. The purified anti-$60\times10^3 M_r$ antibody recognizes only the $60\times10^3 M_r$ protein on Western blots (Fig. 3A), and the anti-$47\times10^3 M_r$ antibody is similarly specific for the $47\times10^3 M_r$ protein (data not shown). The stage-specific immunofluorescence detected with whole serum is obtained with anti-$60\times10^3 M_r$ antibody (detected stages at prophase and telophase are shown in Fig. 3B,C), while affinity-purified anti-$47\times10^3 M_r$ antibody yields no detectable immunofluorescence signal at the concentrations available. This evidence, plus the fact that translocation of immunofluorescence staining during mitosis is continuous and progressive, leads us to conclude that the pattern of indirect immunofluorescent staining reflects physical movement of the $60\times10^3 M_r$ antigen to different loci during mitosis. We hereafter refer to the $60\times10^3 M_r$ protein as TD-60 (for 'Telophase Disc-$60\times10^3 M_r$').

The appearance of TD-60 in strands during translocation to the midzone at mid-anaphase (Fig. 4A) suggests a possible coalignment with interpolar microtubules at this stage. We have confirmed this relationship by double-label immunofluorescence using serum JH and anti-tubulin antibodies (Fig. $4B_1,B_2$). From these data, we believe that microtubules may translocate TD-60 to the midzone of the spindle. Where TD-60 appears in bar-like concentrations during late anaphase (Fig. 4C) and telophase, these also coalign with microtubules.

In the work described here, the confocal microscope was programmed to collect optical sections of about 200 nm through the 10–15 μm depth of field typical of mitotic HeLa cells. All photographs in Figs 1–4 are selected single sections through the middle of a cell interior. Therefore, they definitively demonstrate both the presence of TD-60 internally along the equator of anaphase and telophase cells, and colocalization of TD-60 with microtubules at the midzone. More information can be obtained by analysis of signal in multiple sections from a given cell. Fig. 5A shows a whole cell image generated by digital summation of a series of sections through a single cell. The continuity of TD-60 at the cell equator is quite striking, and TD-60

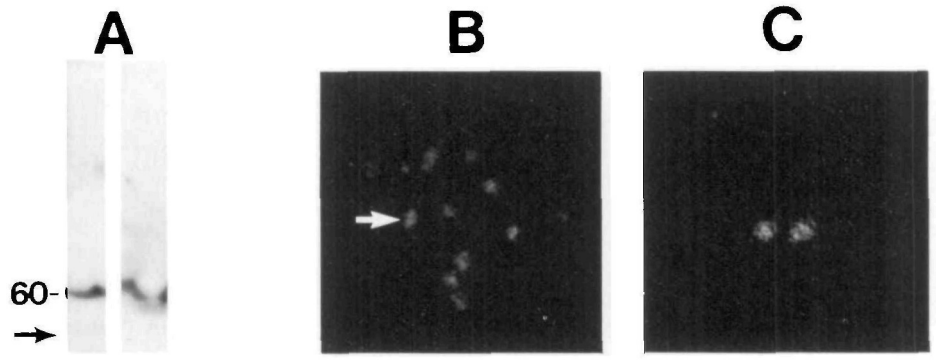

Fig. 3. Affinity purification of anti-TD-60 antibody and demonstration of the presence of TD-60 in centromeres and midbodies. (A) Western blots of chromosomal proteins from MANCA cells were probed with whole JH serum (left lane) or with affinity-purified antibodies (right lane) eluted from nitrocellulose strips containing TD-60. The $47\times10^3 M_r$ antigen recognized by the whole serum is evident in the left lane (arrow). The affinity-purified antibodies rebind only to TD-60. Immunofluorescence with the affinity-purified anti-TD-60 antibodies detects the same mitosis-specific pattern as whole serum, including centromeres (B) in prophase cells, and midbodies (C) following cytokinesis. An arrow (B) indicates a double spot representative of metaphase centromeres. Images were identified as centromeric by colocalization with propidium iodide-stained chromosomes (not shown; see Fig. 2A). Midbodies (C) were identified by their position in recently cleaved cells, as determined with propidium iodide stain (see Fig. 1F).

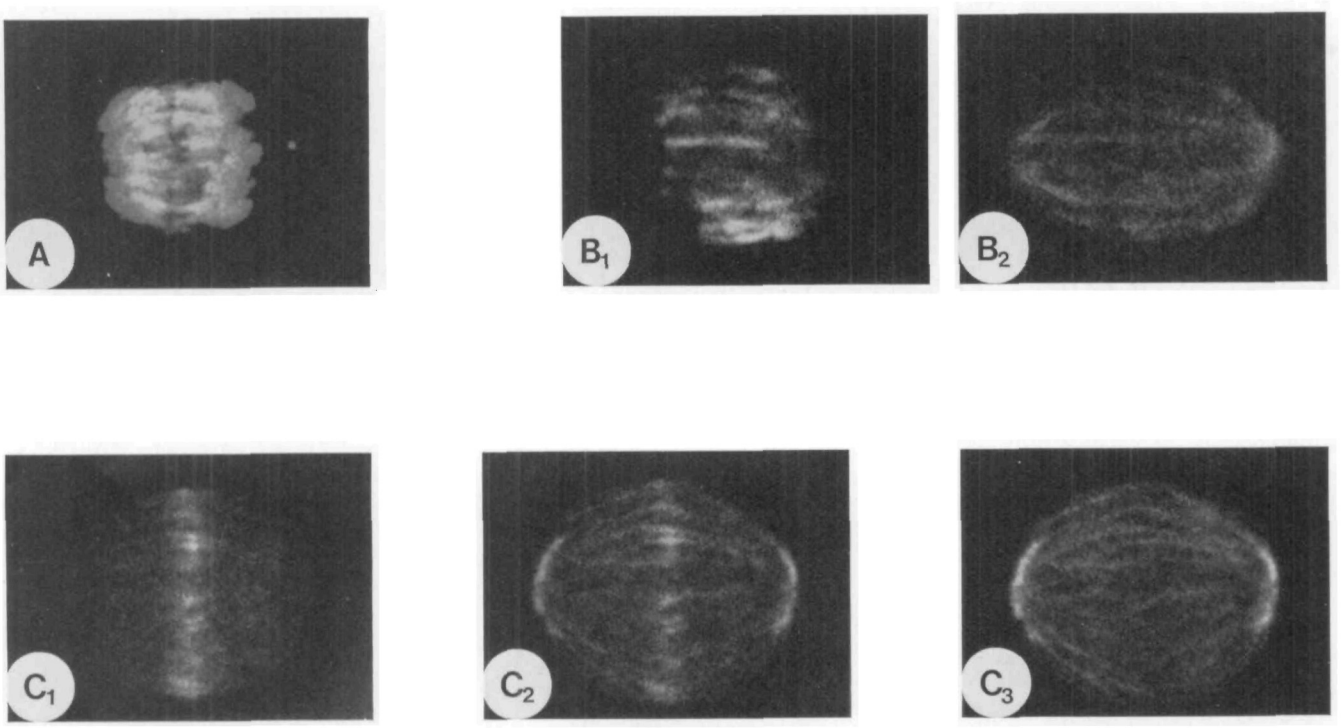

Fig. 4. Co-localization of TD-60 with interpolar spindle microtubules in mid-anaphase. HeLa cells were analyzed for distribution of TD-60 in anaphase. In transition from chromosomes to the midzone of the spindle, TD-60 is present in these cells as linear arrays that bridge between the separating chromosomes, as demonstrated by staining with JH serum antibody (white) compared to the position of chromosomes visualized by propidium iodide (grey) (A). Double immunofluorescent labeling with JH (B_1) and anti-tubulin (B_2) antibodies demonstrates a coalignment of TD-60 with interpolar spindle microtubules during translocation from the chromosomes. TD-60 finally is positioned at the equator of the anaphase spindle, and retains a striated appearance, which coaligns with spindle microtubules at the equator (C). In C, the image of TD-60 alone (C_1), the signals for TD-60 and microtubules merged (C_2), and microtubules alone (C_3) are shown. All images are horizontal optical sections through the middle of the cells.

clearly extends past the lateral boundary of the spindle to the equatorial membrane.

Importantly, the antigen spans the entire midzone in each section (a central section is shown in Fig. 5B). The three-dimensional resolution capacity of confocal microscopy unequivocally demonstrates that TD-60 ultimately participates in a continuous disc that fully partitions the cell throughout the entire midzone plane during late anaphase. These images have been recorded from HeLa cells, but all mammalian cells thus far examined (BHK cells, bovine aortic endothelial cells, mouse 3T3 cells, CHO cells) exhibit the same three-dimensional disc at the spindle equator (data not shown).

TD-60 is an element of an independent organelle

TD-60 appears to translocate on microtubules, then disperse outward to the cell cortex in anaphase. To test the independence of the fully deployed equatorial mitotic disc from microtubules, and hence its existence as an independent organelle, we disassembled microtubules by chilling cells prior to fixation for immunofluorescence. In HeLa cells, cold-disruption is essentially complete for all microtubules (R. L. Margolis, unpublished observations). TD-60 antigen remains in a midzone disc in both late anaphase and telophase cells (Fig. $6A_1,A_2,A_3$) in the absence of microtubules. Without microtubules, distribution of the TD-60 antigen within the disc becomes more uniform (Fig. $6A_1,A_2$), although a bar-like distribution is retained in some cells. Superimposition of signal for the JH serum with that for propidium iodide and anti-tubulin demonstrates that the antigen displays no appreciable diffusion within the cytoplasm following microtubule disassembly (Fig. $6A_3$). In chilled late telophase cells, the antigen remains compactly associated with the midbody (Fig. $6B_1,B_2,B_3$) despite the absence of midbody microtubules. The immunofluorescence intensity of the midzone and midbody is similar to that of unchilled cells at the same stages of mitosis. The existence of the telophase disc as an independent organelle is further reinforced by its resistance to dispersion upon cell lysis. In cells lysed in 85 mM Pipes buffer with 0.2% Triton X-100 following chilling to disassemble microtubules, TD-60 antigen remains at midzones (Fig. $7A_1,A_2$) and midbodies (Fig. $7B_1,B_2$) as a discrete element. These striking results suggest that TD-60 becomes part of an independent organelle that has formed at the midzone of the spindle.

TD-60 distribution in dihydrocytochalasin B-treated cells

Given the position of the element containing TD-60, we have considered that the organelle described above may have a function in cell furrowing. This possibility prompted examination of antigen distribution in cells treated with dihydrocytochalasin B (DCB). DCB is a cytochalasin derivative with high specificity for actin (Atlas and Lin, 1978), which, like other members of the cytochalasin family, induces the formation of binucleate cells (Atlas and Lin, 1978; also see Fig. 8).

To our surprise, we found that HeLa cells recovering from nocodazole blockage in DCB form complete furrows and normal midbodies (Fig. 9) at DCB concentrations up to 20 μM, a concentration 20-fold that required for the

induction of binucleate cells (Carter, 1967; Atlas and Lin, 1978; and data not shown). However, the cells are not impervious to DCB. At 2 μM DCB, cells are clearly affected by the drug. Interphase cells in the population show no stress fibers (data not shown) and the population eventually becomes binucleate as expected (see below). Further, even furrowing cells show the dramatic blebbing (Fig. $9B_2$, indicated by arrows) characteristic of cytochalasin-treated cells (Krishan, 1972). Complete furrowing of mammalian cells in the presence of cytochalasin B, a related drug with affects upon membrane transport and metabolism as well as upon actin assembly, has previously been noted (Krishan, 1972; Sanger and Holtzer, 1972).

We have quantitated the capacity of a population of DCB-treated HeLa cells to cleave. To do this, we generated a population enriched in mitotic HeLa cells by nocodazole arrest, then released the cells into fresh medium, or into medium containing 2 μM DCB and recorded the cleavage morphology of the population at time points. Fig. 8A plots, as a function of time after release from nocodazole arrest, the percentage of initial mitotic cells forming complete furrows with midbodies, and the percentage of binucleate cells. Throughout 120 min of recovery, similar numbers of midbodies are formed in control and DCB-treated cells.

Further, in DCB-treated cells released from nocodazole block for up to 120 min we find an essentially unaltered distribution of TD-60 as compared to control cells. At late anaphase, TD-60 participates in an equatorial disc that spans the diameter of the cell, with some bar-like regions of higher antigen concentration (Fig. $9A_1,A_2$). In telophase cells, the disc remains centered on the developing furrow and contains TD-60 distributed as a series of bars (Fig. $9B_1,B_2$). In completely furrowed DCB cells, the antigen is associated with a midbody of normal appearance (Fig. $9C_1,C_2$). Although the disc containing TD-60 is occasionally displaced from the mid-position of DCB-treated cells, as in the example shown here (Fig. $9A_1,A_2$), in such cases the disc nonetheless remains evenly spaced between the separated chromatids. The disc then becomes aligned with a furrow equidistant from the chromatid sets, yielding an uneven distribution of cytoplasm to the daughter cells (Fig. $9C_1,C_2$).

In cell populations that have recovered from nocodazole for periods longer than 120 min, fewer midbodies are visible in the DCB-treated cells than cleaved controls. By 180 min, completely cleaved DCB-treated cells are 20% less abundant than fully cleaved controls. This dropoff is fully reciprocal to an increase in DCB-treated binucleate cells, which begin to appear at 150 min. Binucleate cells continue to accumulate in DCB, and represent 70% of the initial mitotic population by 6 h of recovery (Fig. 8B). In contrast, a low level of binucleate cells occurs in the control HeLa population, with a maximum of 4% at late times in recovery. For all cells, the recorded maxima relative to initial nocodazole-blocked cells do not approach 100% because of incomplete recovery from nocodazole arrest (Fig. 8).

In cell populations recovering from nocodazole in 2 μM DCB for periods longer than 120 min, when we begin to detect binucleate cell formation, TD-60 distribution is reproducibly altered relative to controls. One regularly finds binucleate cells in which a midbody is displaced within the cytoplasmic space (Fig. $9D_1,D_2$). Such cells are transitory; they appear in early stages of binucleate cell formation, and reach a peak of about 30% of the binucleate population at approximately 180 min (data not shown). These binucleate cells with midbodies are presumably intermediates in the formation of later binucleate populations lacking midbodies. TD-60 apparently degrades completely (or its recognized epitopes are altered) after relapse of the plasma membrane, since no TD-60 is detectable in binucleate cells without midbodies.

The apparent capacity of HeLa cells to cleave in DCB raised the question of the presence of actin and myosin in the region of the cleavage furrow in these drug-treated cells. We have examined these cleaving cells with fluorescent phalloidin, which stains actin polymers, and with an antibody specific to cytoplasmic myosin (Fig. 10). Actin occurs along the entire cortex, without clear organization, in the majority of cells cleaving in the presence of DCB, and in a substantial minority (about 30%) of untreated cleaving cells (Fig. $10A_1A_2$). Actin is never evident in the cell interior or on the telophase disc. About 70% of untreated cells show some increased concentration of actin in the cortex near the furrow, in accord with the recent report of Cao and Wang (1990). Focal accumulations of short actin fibers, appearing as tufts, are present throughout the cell cortex at this stage (not shown). However, careful examination of these cells by optical sectioning at the top and bottom of the cleavage furrow has given no evidence of actin fibers organized into a contractile ring (not shown). These data support the possibility that the telophase disc can form and cleavage can occur in the absence of highly organized or abundant actin, but we cannot rule actin out as an important component of the cell cleavage machinery. Indeed we find that higher DCB concentrations will cause a delay in cell cleavage and that high concentrations of cytochalasin D will arrest cleavage completely (data not shown). After midbody formation is complete, we find that actin accumulates strongly on the proximal surfaces of the two daughter cells (Fig. $10B_1,B_2$). This accumulation of actin following cleavage is inhibited by cytochalasin (not shown). As DCB-treated cells revert to a binucleate state in early interphase, this observation suggests that actin may play a role in maintaining cell cleavage following furrow formation.

In contrast to actin, myosin is clearly organized in cleaving HeLa cells, either in the presence (Fig. 10C) or absence (not shown) of DCB, and it occurs in the cell interior as well as on the cell cortex in the position of the cleavage furrow. Optical sections demonstrate that myosin occurs internally at the cell equator in cleaving DCB-treated cells and that myosin is nearly coincident with TD-60 in these cells (Fig. $10C_1,C_2$). In the absence of DCB, myosin also appears in the cell interior at the position of the telophase disc, but appears more concentrated near the intersection of the disc with the cell cortex (not shown).

We conclude that a telophase disc organelle is generated at the equatorial position of the mitotic spindle in anaphase cells, and that this disc organelle contains a 60×10^3 M_r antigen, TD-60, and probably also myosin. The presence of myosin suggests the intriguing possibility that the telophase disc forms part of the mechanochemical apparatus for cleavage of mammalian cells and that cell cleavage may result from the interaction of disc-associated myosin with cell cortex-associated actin (Fig. 11).

Discussion

We have discovered the presence of a disc organelle that fully bisects the late anaphase cell. This organelle, which we designate the 'telophase disc,' may be involved in the

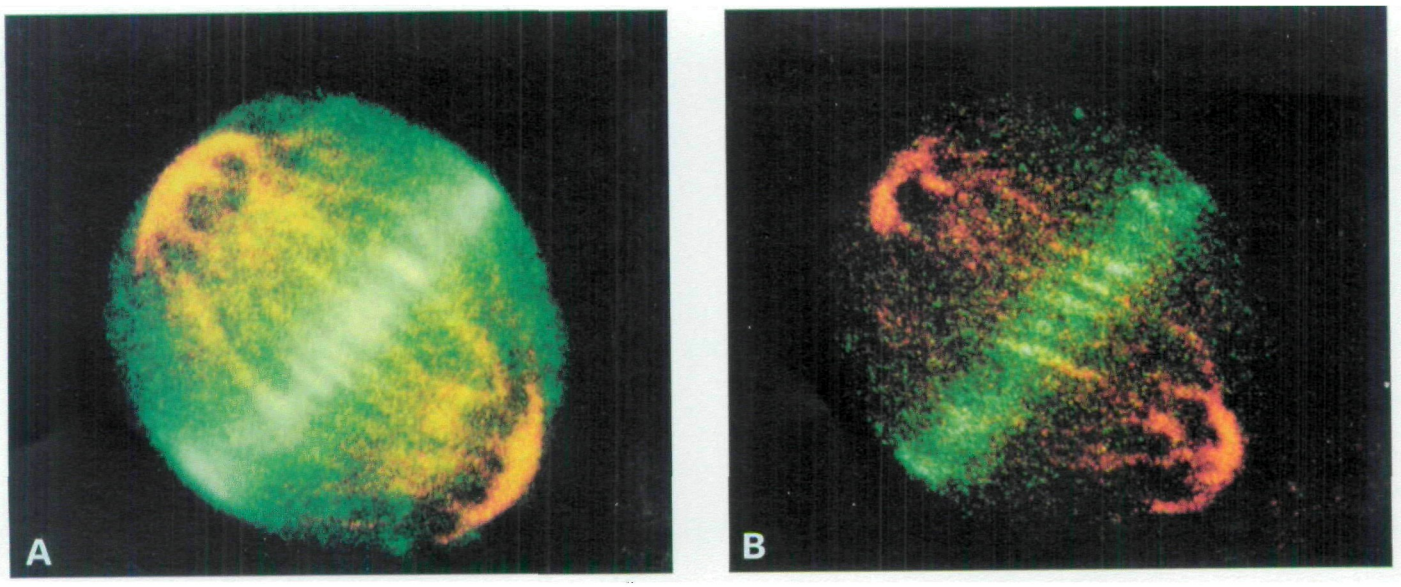

Fig. 5. Formation of a telophase disc that bisects the late anaphase cell at the spindle equator. In late anaphase the TD-60 antigen participates in formation of a continuous disc structure that fully bisects the cell. A whole cell image created by summing horizontal sections of a late anaphase cell is shown (A). In the whole cell image, TD-60 (green; white where intense) is apparent as an equatorial bar that spans the entire cell, well beyond the boundaries of the anaphase spindle (visualized with anti-tubulin, red). The whole cell image has been computer intensified to enhance the background, to show the disc position relative to the whole cell. A central horizontal section of the same cell (B) shows that the TD-60 (green) is evident at the equator in interior cell sections. It therefore represents an element of a continuous disc bisecting the late anaphase cell. ×3100.

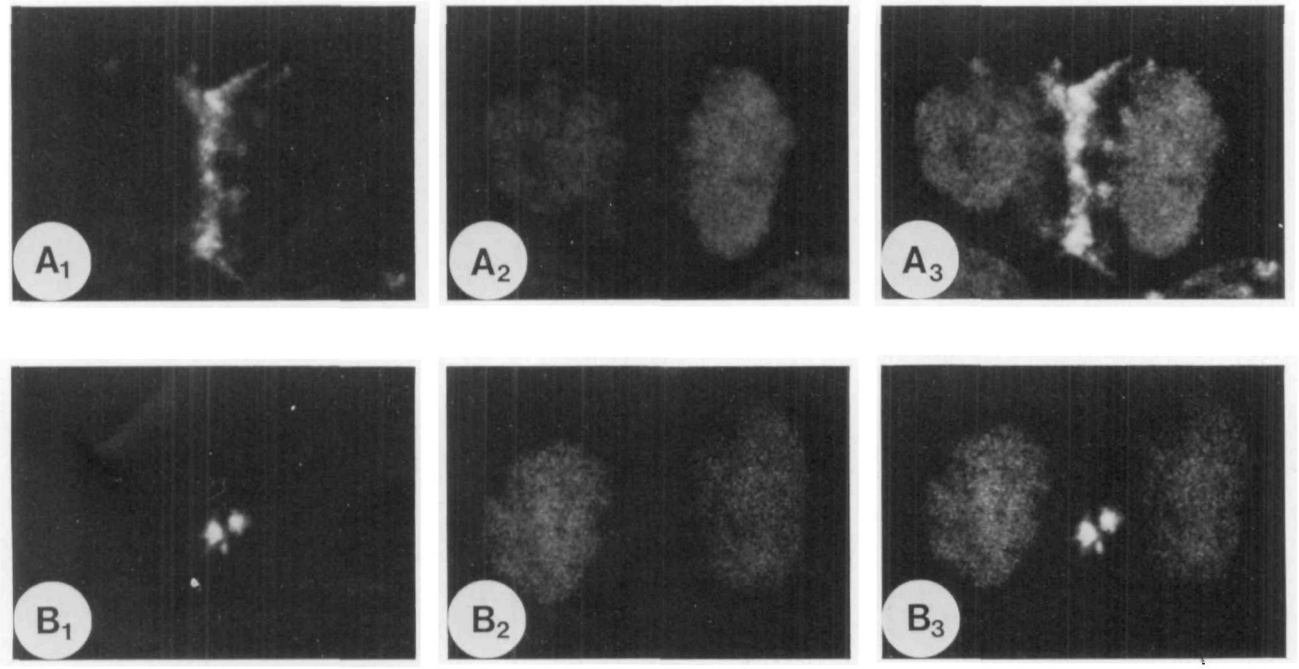

Fig. 6. The telophase disc and midbody are independent of the continued presence of microtubules. HeLa cells were blocked with nocodazole overnight, released from blockage for 65 min, then chilled on ice for 30 min. (A) Following removal of microtubules by chilling, TD-60 remains spanning the equator of early telophase cells, as shown by a central optical section of such a cell. (A_1) TD-60 antigen alone; (A_2) the same optical section stained both with anti-tubulin antibody (detected by Texas Red-conjugated secondary antibodies) and with propidium iodide; (A_3) the merged image of TD-60, propidium iodide and tubulin. (B) At the midbody stage TD-60 (B_1) persists after chilling, despite the fact that microtubules (B_2) in the midbody have been disassembled by chilling. All conditions and stains in B are as in A.

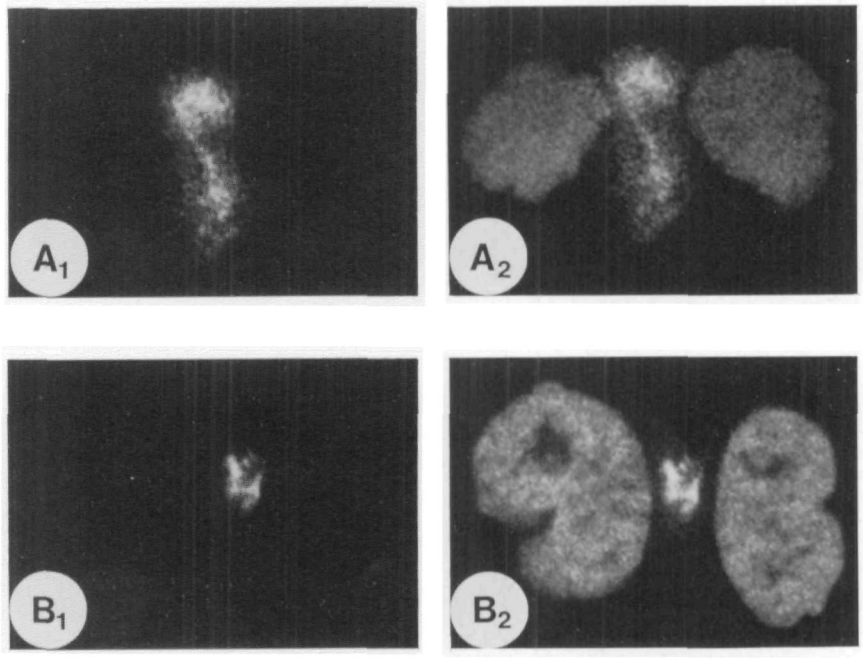

Fig. 7. The telophase disc persists after both chilling and permeabilizing cells. HeLa cells in mitosis were chilled and lysed to demonstrate the stability of the telophase disc to these treatments. (A) A late anaphase cell. At left (A_1) is the signal for TD-60 alone, detected with JH serum; at right (A_2) is the image for TD-60 merged with the image for anti-tubulin antibody and propidium iodide. As in Fig. 5, microtubules are absent. (B) Two interphase cells are shown with TD-60 remaining at a midbody. HeLa cells were enriched for late mitotic population by blockage in nocodazole, followed by shakeoff of mitotic cells. These cells were then permitted to recover in spinner culture for 65 min. Cells were then centrifuged onto polylysine-coated coverslips, chilled on ice for 30 min, then permeabilized by exposure to 0.2% Triton X-100 in 85 mM Pipes on ice for 10 min. All images represent horizontal optical sections through cells by confocal microscopy.

mechanism of cell cleavage. The disc organelle was detected through use of an antibody that recognizes a mitosis-specific antigen, TD-60, and through confocal microscopy, which permits three-dimensional analysis of cells by optical sectioning. TD-60 is first strongly evident during prophase, when it is preferentially located at the centromeric regions of chromosomes. TD-60 remains on chromosomes until mid-anaphase, then undergoes a series of translocations, moving first to microtubules that lie between the two separating chromatid sets, and then to an equatorial disc that appears at the midzone of the spindle just prior to furrow formation. On the basis of the disc's stability, despite microtubule disassembly and cell lysis, we conclude that the antigen becomes part of an organelle that forms in anaphase. The organelle completely partitions the cell at the spindle equator in late anaphase, is

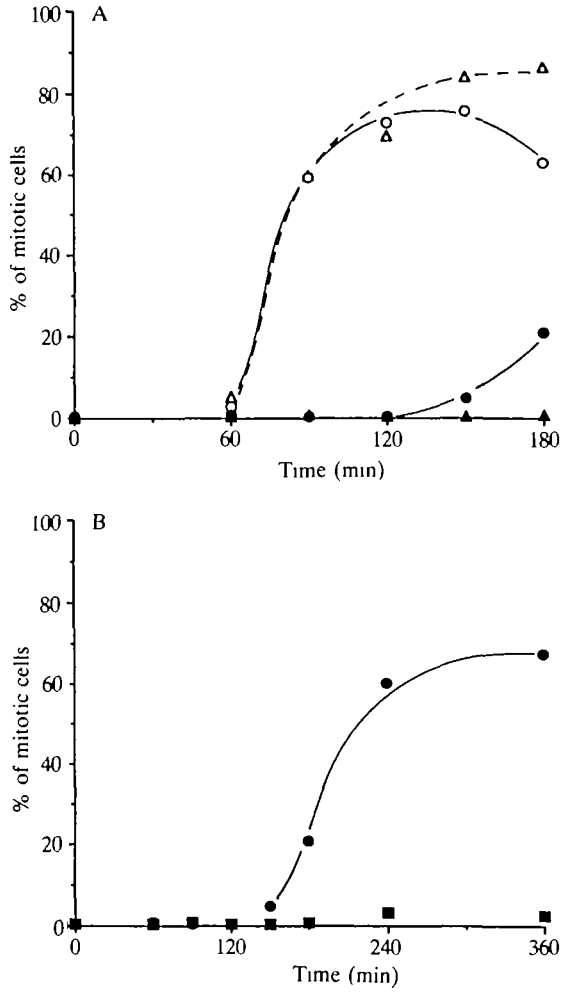

Fig. 8. Time course and extent of complete cell cleavage following treatment with dihydrocytochalasin B. HeLa cells were synchronized with a double thymidine block and then arrested with nocodazole for 12 h to generate a population of 80% mitotic cells. Cells were then permitted to recover from nocodazole block (time 0), in either the presence or absence of 2 μM dihydrocytochalasin B (DCB). (A) Cells were scored for complete cleavage, defined by the presence of a midbody (detected with serum JH) and a complete furrow; (△——△) complete cleavage of control cells; (○——○) complete cleavage of DCB-treated cells. The percentage of binucleate cells in the population, defined as cells with two nuclei and no cleavage furrow apparent, was also recorded. (▲——▲) binucleate control cells; (●——●) binucleate DCB-treated cells. (B) Binucleate cell formation was followed to later times. (■——■) Control cells; (●——●) DCB-treated cells. The ordinate represents the percentage of cells of the particular morphology relative to the population frequency (time=0) of the original blocked mitotic population (typically 80% of all cells), as described in Materials and methods.

centered on the forming furrow in telophase, and is apparently unaltered as cells undergo cleavage in the presence of dihydrocytochalasin B. These data suggest the possibility that the telophase disc organelle functions in the mechanics of cytokinesis.

TD-60 is present on isolated chromosomes, as demonstrated by Western blot analysis of purified chromosomes derived from nocodazole-blocked cells. The continuity of the immunofluorescence pattern as the antigen translocates from site to site in mitosis, and the detection of prophase centromeres and midbodies by affinity-purified TD-60 antibody, indicates that TD-60 is the antigen responsible for the immunofluorescence images generated throughout mitosis.

Distribution of TD-60

During anaphase B, antiparallel microtubules slide apart to form a narrow zone of overlap, which is equidistant from the spindle poles and defines the midzone of the spindle in mammalian culture cells. Other midzone antigens have been described that localize to the equatorial plane of anaphase and telophase cells, and finally collect in the midbody (Cooke *et al.* 1987; Kingwell *et al.* 1987; Sellitto and Kuriyama, 1988). TD-60 is novel among known midzone antigens both in the time course of its arrival at the spindle midzone, and in its extension into a microtubule-independent disc that completely bisects the cell at the onset of cleavage.

INCENPs (*In*ner *Cen*tromere *P*roteins), midzone antigens of 135 and 155×10^3 M_r, are detected in chicken cells using a monoclonal antibody (Cooke *et al.* 1987). In prophase, INCENPs occur on chromosomes along the axis separating the sister chromatids, with an enrichment at centromeres. In contrast, TD-60 is present as a single focus at the chromosome primary constriction. Whereas INCENPs remain at the spindle midzone position as sister chromatids separate in anaphase, TD-60 remains with the separating chromatids until mid-anaphase. INCENPs come to lie proximal to the plasma membrane during furrowing, but published images suggest this association is generated by the approach of the furrow to the midzone spindle remnant in telophase (Cooke *et al.* 1987). In contrast, TD-60 extends to the full diameter of the cell, well beyond the position of the mitotic spindle, prior to furrowing. Kingwell *et al.* (1987) reported an apparently mitosis-specific mammalian antigen of 38×10^3 M_r with a distribution pattern similar to INCENPs. The 38×10^3 M_r antigen, recognized by a human autoimmune serum, is also clearly distinct from TD-60 in both size and distribution.

The mammalian CHO1 antigens (Sellitto and Kuriyama, 1988) represent another distinct set of midzone proteins. Unlike TD-60, these antigens of 95 and 115×10^3 M_r show no apparent association with chromosomes during metaphase or anaphase. Instead, they are present from metaphase onward as a region of the central spindle that probably corresponds to the overlap zone of interpolar microtubules. Further, as anaphase proceeds, the CHO1 antigens show no reported colocalization with the cell membrane at the spindle equator, either in anaphase or telophase.

Since TD-60 remains with separating sister chromatids through early anaphase, it is temporally the last of the known spindle antigens to arrive at the midzone. Incorporation of antigens to the region of spindle overlap at different times in mitosis could permit the midzone to have multiple temporally distinct functions. The midzone may direct spindle organization during early mitosis (Sellitto and Kuriyama, 1988), serve as a site of mechanochemical motor function during anaphase B (Wordeman *et al.* 1987), and position an organelle for cell cleavage during telophase (Cooke *et al.* 1987). Since TD-60 remains associated with chromosomes following sister chromatid dissociation, it appears possible that the centromeric region sequesters TD-60 for later deposition at the midzone in response to a mid-anaphase signal.

When it dissociates from the chromosomes in mid-anaphase, TD-60 shows coalignment with microtubules,

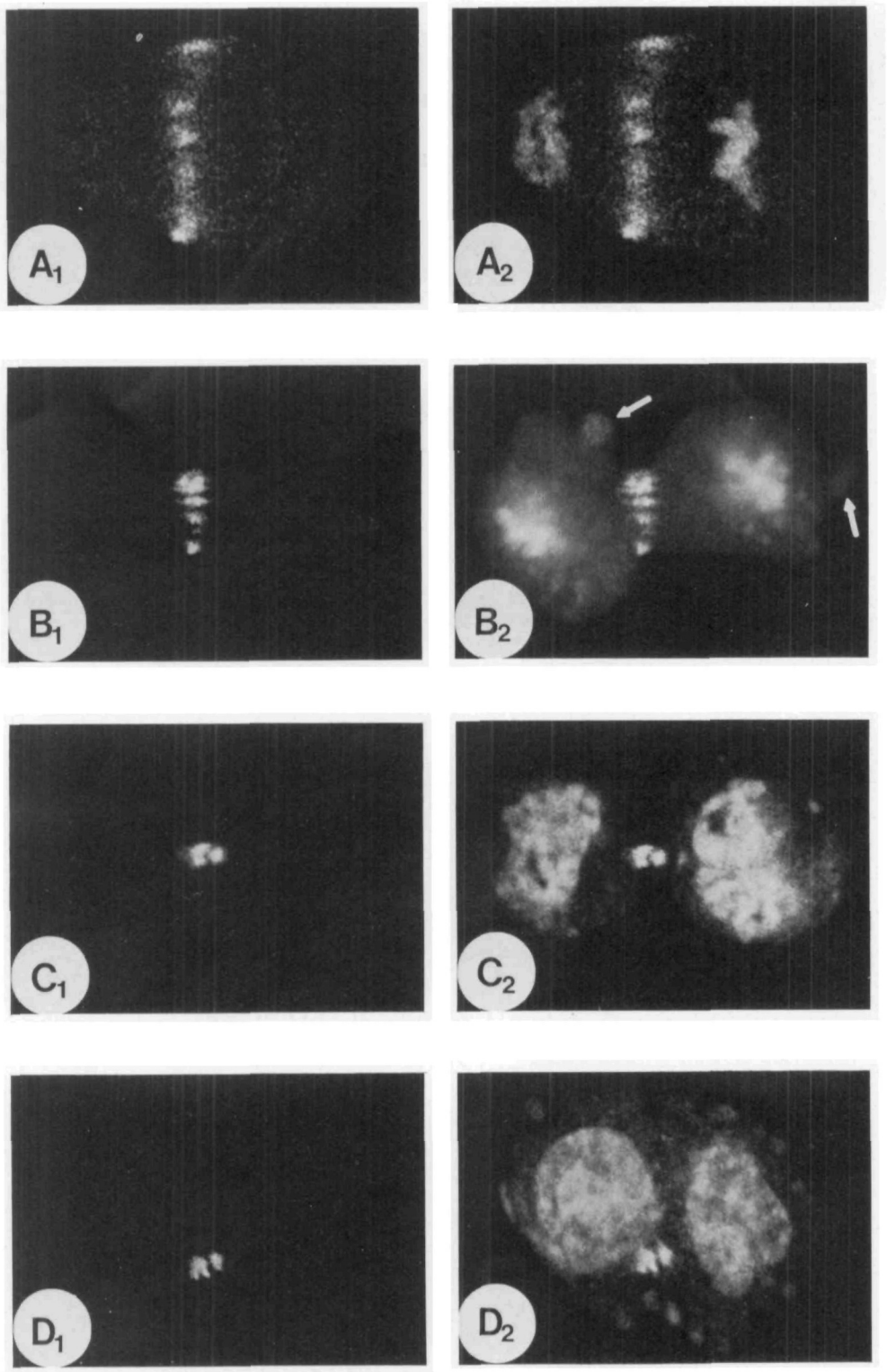

Fig. 9. Immunofluorescence localization of TD-60 in cells undergoing cleavage in dihydrocytochalasin B. HeLa cells were blocked for 12 h in nocodazole, and permitted to recover in medium containing 10 μM DCB. At 60 and 90 min of recovery, cells were fixed and processed for immunofluorescence with JH serum, and counterstained with propidium iodide. At late anaphase (A_1,A_2) TD-60 spans the cell equator. In mid-telophase cells (B_1,B_2), TD-60 bridges the cell at the furrowing membrane. Notice that furrowing proceeds despite extensive blebbing (arrows) and deformation of the cell resulting from DCB treatment. Cells with complete furrows and midbodies (C_1,C_2) of normal appearance form in the presence of DCB. Finally, binucleate cells with midbodies in the cytoplasm are transiently seen (D_1,D_2). The left column shows TD-60 localization alone; the right column shows the TD-60 image merged with the propidium iodide signal. All images represent horizontal optical sections through cells by confocal microscopy.

but only in the region between the sister chromatids. It appears that microtubules are involved transitionally in the migration of TD-60 to the equator, whereupon it becomes incorporated into a microtubule-independent organelle. Perhaps, in transit to the spindle equator in anaphase, TD-60 becomes incorporated into a complex involving a motor protein that migrates to the plus end of the interpolar microtubules. The CHOl antigens discussed above show a similar tendency to concentrate toward the spindle midzone in anaphase, in association with microtubules (Sellitto and Kuriyama, 1988).

TD-60 as a component of the telophase disc

The telophase disc organelle that incorporates TD-60 forms at the midzone of the spindle in anaphase and telophase. This organelle fully partitions the cell at the spindle equator in late anaphase and through telophase.

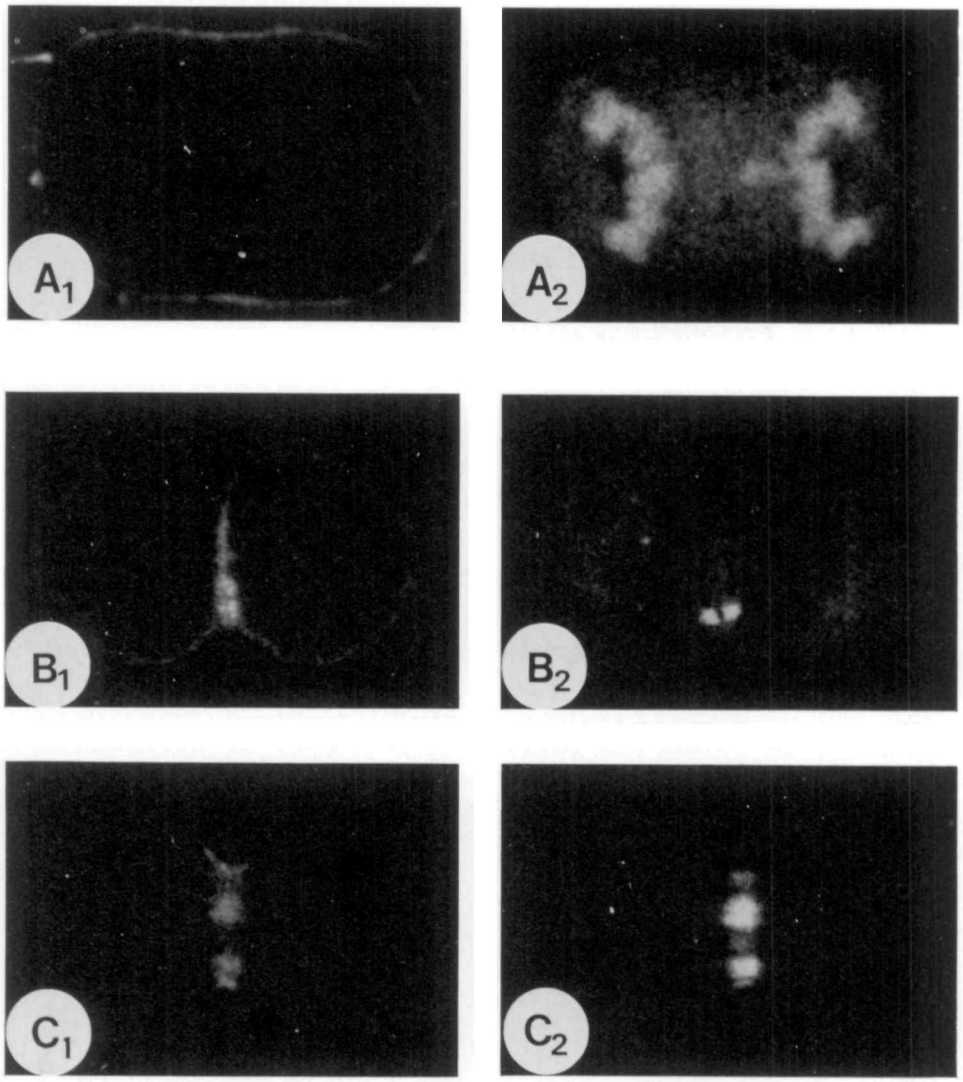

Fig. 10. Localization of actin and myosin in cleaving cells. All images represent 200 nm optical sections of cells by confocal microscopy. Images shown for actin (A and B) are of cells cleaving in the absence of DCB. The image shown for myosin (C) is of a cell cleaving in DCB. Actin, detected with FITC–phalloidin, occurs in largely unorganized aggregates at the cell cortex during cell furrowing in telophase (A_1). Chromosomes are shown in the same cell by counterstain with propidium iodide (A_2). In early interphase, actin (B_1) is strongly concentrated on the apposed membranes of the two daughter cells on either side of the midbody (B_2), detected here with anti-tubulin antibody counterstain. Myosin, detected with primary antimyosin antibody and FITC-conjugated goat anti-mouse secondary antibody (C_1), is present in the approximate position of the telophase disc antigen TD-60 (C_2) in an optical section of a cleaving cell. Myosin occurs, as well, at the cell cortex proximal to the cleavage furrow position.

Evidence that the telophase disc exists as an independent organelle includes continuity of elements of the disc as shown by TD-60 distribution, retention of disc-like organization in the absence of microtubules, and maintenance of an intact disc in permeabilized cells. Strong intermolecular interactions must maintain the telophase disc, since TD-60 does not diffuse throughout the cytoplasm following the removal of microtubules or upon cell lysis. Although other midzone antigens may participate in the organelle structure defined by TD-60, no protein has previously been demonstrated to span the equator of the anaphase cell, or to participate in forming a continuous disc that is microtubule- and actin-independent, and resistant to cell lysis. The observed survival of the telophase disc following microtubule disassembly and cell lysis should ultimately permit conditions to be defined that will permit isolation of the organelle for *in vitro* examination of its components and function.

Possible role for the telophase disc in mammalian cell cytokinesis

The telophase disc forms at the proper place and the appropriate time to play a role in cell cleavage. We propose a model of cytokinesis in which the disc is generated in mammalian cells for the purpose of association with the cell cortex to create the machinery for cleavage. In this model (Fig. 11), the telophase disc spans the equatorial diameter of the anaphase cell and concentrates and aligns myosin at the position where the furrow will form. The disc-associated myosin then interacts with cortical actin, but only at the point of contact where the fully expanded disc meets the cell cortex. The result is that cell cleavage occurs only at the interface where the disc-associated myosin interacts with cortical actin.

This mechanism would assure the following: the position of metaphase chromosomes would determine the position of the cleavage furrow by templating the disc; myosin, present on the disc, would be positioned only where cleavage is required to occur; the disc alone and the cell cortex alone could not create a cleavage event, but must contact each other, and this could only occur when the disc expands during anaphase, thus assuring that the timing of cytokinesis is coupled to events in anaphase.

In our model, cortical actin is required for cytokinesis, but it need not be abundant, nor arranged in an obvious ring structure, nor need it be more concentrated at the furrow than elsewhere in the cortex during cleavage. A cortical ring of actin may be present, but rather than being a specific organelle generated for cell cleavage, it would be caused by the local rearrangement of cortical actin as a result of its association with disc myosin. Thus, cells could

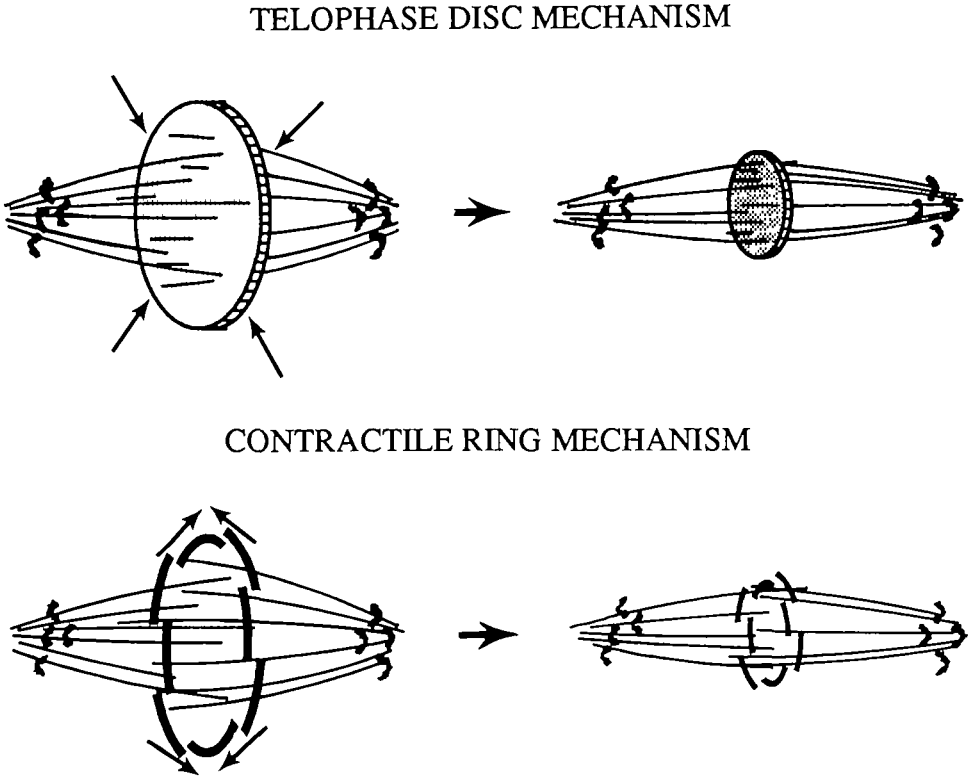

Fig. 11. A proposed mechanism for mammalian cell cleavage due to interaction of the telophase disc with cortical actin. (A) Our proposed mechanism, in which the telophase disc aligns at the mitotic equator in late anaphase and links at its periphery with actin in the cell cortex. The telophase disc, by binding and organizing myosin, limits the furrowing mechanism to the site of juncture between telophase disc myosin and cortical actin (arrowheads). This arrangement allows, but does not require, contraction that is radially inward (arrows) to create cell cleavage. (B) The contractile ring mechanism (Schroeder, 1975), in which actin and myosin have been proposed to align as a ring structure in the cell cortex and constrict the cell through a purse-string (tangential) contraction mechanism.

cleave normally even when actin has been largely depolymerized by dihydrocytochalasin (Figs 8 and 9), since even short cortical 'tufts' of actin would be sufficient to interact effectively with the disc-associated myosin to create a furrow.

This possibility is consistent with evidence in the literature. In echinoderm oocytes, it is evident that microfilaments assume the morphology of an equatorial ring in the furrowing region of the cell cortex (Schroeder, 1968), but there are conflicting reports on whether actin preferentially concentrates to the furrow during cleavage of mammalian cells (Herman and Pollard, 1978; Herman and Pollard, 1979; Aubin *et al.* 1981). In a recent report, Cao and Wang (1990) found a convincing concentration of actin, detected by the F-actin probe phalloidin, in only 15 % of cleaving NRK cells, and we have obtained similar results in HeLa cells.

In keeping with the proposed role of actin in force production, cytochalasin B causes a reversion of furrow formation in sea-urchin oocytes within one minute of application (Schroeder, 1972). However, in apparent contrast to the results obtained with sea-urchin oocytes, deep furrowing prior to the formation of binucleate cells has been observed repeatedly upon exposure of various mammalian cell lines to cytochalasin B or dihydrocytochalasin B (Carter, 1967; Sanger and Holtzer, 1972; Aubin *et al.* 1981). Krishan (1972) demonstrated by time-lapse microscopy that individual mouse L cells treated with cytochalasin B undergo furrowing to form narrow cytoplasmic bridges, and that the plasma membrane subsequently relapses to form binucleate cells. A similar result was obtained in HeLa cells, with 2–3 h elapsing between formation of the furrow and its relaxation (Sanger and Holtzer, 1972). There is no evidence for organized actin in the furrow region of mammalian cells exposed to cytochalasin (Schroeder, 1970), despite their ability to undergo furrowing (Aubin *et al.* 1981).

Preliminary evidence in our laboratory shows that, as in sea-urchin oocytes, some minimal level of assembled actin is required for cytokinesis in mammalian cells. We have found that higher concentrations of dihydrocytochalasin B than used in Fig. 8 will delay cleavage, and that cytochalasin D can fully arrest cleavage in telophase HeLa cells (Andreassen and Margolis, unpublished observations). These results may be interpreted as showing a critical role for actin in cell cleavage, though not necessarily for the formation of a cortical ring.

In contrast to actin, myosin shows a marked concentration at the cleavage furrow at the onset of membrane deformation in a variety of cells from different phyla (Fujiwara and Pollard, 1976; Yumura and Fukui, 1985; Schroeder, 1987). We have found that myosin, like TD-60, is not restricted to the membrane of furrowing cells, but rather can be present throughout the midzone diameter. Our results therefore implicate the telophase disc as determining the observed myosin localization.

The fact that myosin localizes to the telophase disc suggests the possibility that the vector of force in cleavage is radial rather than tangential (as would have been required of a contractile ring). A radial force can explain cleavage in *Drosophila* embryos where the process of cellularization resembles a falling curtain more than a constricting ring (Fullilove and Jacobson, 1971; Warn, 1991), and can explain furrowing that has been reported to occur in cases where there is no coordinate constriction of the cell diameter (Schroeder, 1990).

It is formally possible, as an extreme, that actin and myosin interact within the telophase disc to yield furrowing by a constriction of the disc itself, with a radial vector of force. The possibility of a self-contractile role for the telophase disc would appear less likely than the telophase disc/cortical actin model stated above, since we do not detect F-actin in the midzone interior using confocal microscopy (Fig. 10). If the disc were indeed self-contrac-

tile, it would therefore appear to require myosin interacting with a protein other than F-actin within the disc.

The true role of the telophase disc in cytokinesis awaits analysis of the molecular components and functions of the disc. As a beginning of a molecular analysis, we have found in recent work that overexpression of a T-cell protein tyrosine phosphatase, truncated in its carboxyl-terminal region, results in a majority of transfected BHK cells becoming multinucleate (Cool, Andreassen, Tonks, Fischer, Krebs and Margolis, unpublished data). On examination of cytokinesis in these cells, we find that the telophase disc may show all possible diameters from the anaphase configuration to midbody, while little or no furrowing of the membrane is evident. It appears, therefore, that there has been a dissociation of the telophase disc from the cell membrane at some point during cleavage. We interpret these results as demonstrating a requirement for tyrosine phosphorylation in order to maintain a link from the disc to the cell cortex for the purpose of generating cell cleavage. We expect that critical evaluation of cytokinesis in these tyrosine phosphatase overexpressing cells will be of value in ascertaining whether the function of the telophase disc is as modeled here.

We thank Paul Goodwin and Straton Spyropoulos for assistance in image analysis, and Pam Noble for secretarial assistance. We also thank Dr William Earnshaw (Johns Hopkins) for the gift of CENP-B antibodies, and Dr Tom Pollard and Don Kaiser (Johns Hopkins) for supplying the myosin antibodies. This work was supported by NIH GM 32022 and by a grant from MDA.

References

Atlas, S. J. and Lin, S. (1978). Dihydrocytochalasin B, biological effects and binding to 3T3 cells. *J. Cell Biol.* **76**, 360–370.

Aubin, J. E., Osborn, M. and Weber, K. (1981). Inhibition of cytokinesis and altered contractile ring morphology induced by cytochalasins in synchronized PtK_2 cells. *Expl Cell Res.* **136**, 63–79.

Buck, R. C. and Tisdale, J. M (1962). The fine structure of the midbody of the rat erythroblast. *J. Cell Biol.* **13**, 109–115.

Cao, L.-G. and Wang, Y.-L. (1990). Mechanism of the formation of contractile ring in dividing cultured mammalian cells. II. Cortical movement of microinjected actin filaments. *J. Cell Biol.* **110**, 1089–1095.

Carter, S. B (1967). Effects of cytochalasins on mammalian cells. *Nature* **213**, 261–264.

Cooke, C. A., Heck, M. S. and Earnshaw, W. C. (1987). The inner centromere protein (INCENP) antigens. movement from inner centromere to midbody during mitosis. *J. Cell Biol.* **105**, 2053–2067

Earnshaw, W. C., Halligan, N., Cooke, C. and Rothfield, N. (1984). The kinetochore is part of the metaphase chromosome scaffold. *J. Cell Biol* **98**, 352–357.

Earnshaw, W C , Sullivan, K. F., Machlin, P. S., Cooke, C. A., Kaiser, D. A., Pollard, T D., Rothfield, N. F. and Cleveland, D. W. (1987). Molecular cloning of cDNA for CENP-B, the major human centromere autoantigen. *J. Cell Biol.* **104**, 817–829

Fujiwara, K and Pollard, T. D. (1976). Fluorescent antibody localization of myosin in the cytoplasm, cleavage furrow, and mitotic spindle of human cells. *J. Cell Biol.* **71**, 848–875

Fullilove, S L. and Jacobson, A. G. (1971). Nuclear elongation and cytokinesis in *Drosophila montana*. *Devl Biol.* **26**, 560–577.

Herman, I. M. and Pollard, T D. (1978). Actin localization in fixed dividing cells stained with fluorescent heavy meromyosin. *Expl Cell Res.* **114**, 15–25.

Herman, I. M. and Pollard, T. D. (1979). Comparision of purified anti-actin and fluorescent heavy meromyosin staining patterns in dividing cells. *J. Cell Biol.* **80**, 509–520.

Johnson, G. D., Davidson, R. S , McNamee, K. C., Russell, G , Goodwin, D. and Holborow, E. J. (1982). Fading of immunofluorescence during microscopy, a study of the phenomenon and its remedy. *J. Immun. Meth.* **55**, 231–242.

Kingwell, B., Fritzler, M. J., Decoteau, J. and Rattner, J. B. (1987). Identification and characterization of a protein associated with the stembody using autoimmune sera from patients with systemic sclerosis. *Cell Motil. Cytoskel.* **8**, 360–367.

Krishan, A (1972). Cytochalasin B, time lapse cinematographic studies on its effects on cytokinesis. *J. Cell Biol.* **54**, 657–664.

Lewis, C. D. and Laemmli, U. K. (1982). Higher order metaphase chromosome structure: evidence for metalloprotein interactions. *Cell* **29**, 171–181.

Lima-de-Faria, A. (1955). The division cycle of the kinetochore. *Hereditas* **41**, 238–240.

McIntosh, J. R. and Landis, S. C. (1971). The distribution of spindle microtubules during mitosis in cultured human cells. *J. Cell Biol.* **49**, 468–497.

Nishikori, M., Hansen, H., Jhanwar, S., Fried, J., Sordillo, P , Koziner, B., Lloyd, K. and Clarkson, B. (1984). Establishment of a near tetraploid B-cell lymphoma line with duplication of the 8;14 translocation *Cancer Genet. Cytogenet.* **12**, 39–50

Sanger, J. W and Holtzer, H. (1972). Cytochalasin B: effects on cytokinesis, glycogen, and ^{3}H-D-glucose incorporation. *Am. J Anat.* **135**, 293–298.

Schroeder, T. E. (1968). Cytokinesis, filaments in the cleavage furrow. *Expl Cell Res.* **53**, 272–276

Schroeder, T. E. (1970). The contractile ring. I. Fine structure of dividing mammalian (HeLa) cells and the effects of cytochalasin B. *Z. Zellforsch mikrosk. Anat.* **109**, 431–449.

Schroeder, T. E. (1972). The contractile ring. II. Determining its brief existence, volumetric changes, and vital role in cleaving *Arbacia* eggs. *J. Cell Biol.* **53**, 419–434.

Schroeder, T. E (1975). Dynamics of the contractile ring. In *Molecules and Cell Movement* (ed. S. Inoue and R. E. Stephens), pp. 305–335. New York: Raven Press.

Schroeder, T. E. (1987). Fourth cleavage of sea urchin blastomeres, microtubule patterns and myosin localization in equal and unequal cell divisions. *Devl Biol.* **124**, 9–22.

Schroeder, T. E. (1990). The contractile ring and furrowing in dividing cells. *Ann. N.Y. Acad. Sci.* **582**, 78–87.

Sellitto, C. and Kuriyama, R (1988). Distribution of a matrix component of the midbody during the cell cycle in chinese hamster ovary cells. *J. Cell Biol.* **106**, 431–439.

Sheir-Neiss, G., Lai, M. H. and Morris, N. R. (1978). Identification of a gene for β-tubulin in Aspergillus nidulans. *Cell* **15**, 639–647.

Sunkara, P S., Wright, D A. and Rao, P. N. (1979). Mitotic factors from mammalian cells induce germinal vesicle breakdown and chromosome condensation in amphibian oocytes. *Proc natn. Acad. Sci. U.S A.* **76**, 2799–2802.

Towbin, H., Staehelin, T. and Gordon, J. (1979). Electrophoretic transfer of proteins from polyacrylamide gels to nitrocellulose sheets: procedures and some applications. *Proc. natn. Acad Sci. U.S.A.* **76**, 4350–4354.

Warn, R. M. (1991). Cytokinesis genetics takes wing. *Trends Genet.* **6**, 309–310

Wordeman, L., Masuda, H. and Cande, W. Z. (1989). Distribution of a thiophosphorylated spindle midzone antigen during spindle reactivation *in vitro*. *J. Cell Sci.* **93**, 279–285.

Yumura, S. and Fukui, Y. (1985). Reversible cyclic AMP-dependent change in distribution of myosin thick filaments in *Dictyostelium*. *Nature* **314**, 194–196.

(Received 18 February 1991 – Accepted, in revised form, 26 April 1991)